J|A|C|S
ARTICLES

Published on Web 11/05/2009

Nanowire Crystals of a Rigid Rod Conjugated Polymer

Huanli Dong,[†,§] Shidong Jiang,[†,§] Lang Jiang,[†,§] Yaling Liu,[‡] Hongxiang Li,[†] Wenping Hu,[*,†] Erjing Wang,[†,§] Shouke Yan,[*,†] Zhongming Wei,[†,§] Wei Xu,[†] and Xiong Gong[*,||]

Beijing National Laboratory for Molecular Sciences, Key Laboratory of Organic Solids and State Key Laboratory of Polymer Physics & Chemistry, Institute of Chemistry, Chinese Academy of Sciences (CAS), Beijing 100190, China, National Center for Nanoscience and Technology, Beijing 100190, China, Graduate University of CAS, Beijing 100039, China, and Center for Polymers and Organic Solids, University of California at Santa Barbara, Santa Barbara, California 93106

Received August 19, 2009; E-mail: huwp@iccas.ac.cn; skyan@mail.buct.edu.cn; xgong@physics.ucsb.edu

Abstract: In this paper, we show that well-defined, highly crystalline nanowires of a rigid rod conjugated polymer, a poly(*para*-phenylene ethynylene)s derivative with thioacetate end groups (TA-PPE), can be obtained by self-assembling from a dilute solution. Structural analyses demonstrate the nanowires with an orthorhombic crystal unit cell wherein the lattice parameters are $a \approx 13.63$ Å, $b \approx 7.62$ Å, and $c \approx 5.12$ Å; in the nanowires the backbones of TA-PPE chains are parallel to the nanowire long axis with their side chains standing on the substrate. The transport properties of the nanowires examined by organic field-effect transistors (OFETs) suggest the highest charge carrier mobility approaches 0.1 $cm^2/(V\ s)$ with an average value at $\sim 10^{-2}$ $cm^2/(V\ s)$, which is 3−4 orders higher than that of thin film transistors made by the same polymer, indicating the high performance of the one-dimensional polymer nanowire crystals. These results are particular intriguing and valuable for both examining the intrinsic properties of PPEs polymer semiconductors and advancing their potential applications in electronic devices.

Introduction

One-dimensional (1D) nanostructures, such as nanowires, nanotubes, and nanofibers, have attracted particular interest due to their unique electronic and optical properties.[1] It is especially true for single crystalline nanowires because single crystals indeed reveal intrinsic properties of materials and open up prospects for high quality devices and circuits. Organic single crystals of small molecular weight materials[2] have demonstrated this point. However, to date, crystals of conjugated polymers have been rarely addressed[3] regardless of their great advantages in solution-process, large area device fabrications, mechanical flexibility, and the incorporation of functionality by molecular design. Therefore, the obtainment of high-quality, single crystalline polymer nanowires for the study of intrinsic charge-transport properties of polymer semiconductors and realization of high-performance polymer electronic devices remain challenging.

While a variety of methods have been developed for the fabrication of polymer nanostructures including solution chemistry,[4a,b] direct writing,[4c] electrospinning,[4d] templates and templateless assembly,[4e−g] and so forth,[4] the quality, structure, and properties of the resulted polymer nanostructures are related not only to the preparation process but also closely to the polymer molecular structures, which to some extent strongly influences the intermolecular interactions and then the growth types of nanostructures.[3,4] In general, ideal molecular structures together with proper experimental conditions are key require-

[†] CAS.
[§] Graduate University of CAS.
[||] University of California at Santa Barbara.
[‡] National Center for Nanoscience and Technology.

(1) (a) Wu, Y.; Xiang, J.; Yang, C.; Lu, W.; Lieber, C. M. *Nature* **2004**, *430*, 61–65. (b) Wang, J. F.; Gudiksen, M. S.; Duan, X. F.; Cui, Y.; Lieber, C. M. *Science* **2001**, *293*, 1455–1457. (c) Javey, A.; Guo, J.; Wang, Q.; Lundstrom, M.; Dai, H. *Nature* **2003**, *424*, 654–657. (d) Beckman, R.; Johnston-Halperin, E.; Luo, Y.; Green, J. E.; Heath, J. R. *Science* **2005**, *310*, 465–468. (e) Hochbaum, A. I.; Chen, R.; Delgado, R. D.; Liang, W.; Garnett, E. C.; Najarian, M.; Majumdar, A.; Yang, P. *Nature* **2008**, *451*, 163–167.

(2) (a) Sundar, V. C.; Zaumseil, J.; Podzorov, V.; Menard, E.; Willett, R. L.; Someya, T.; Gershenson, M. E.; Rogers, J. A. *Science* **2004**, *303*, 1644–1646. (b) Mas-Torrent, M.; Durkut, M.; Hadley, P.; Ribas, X.; Rovira, C. *J. Am. Chem. Soc.* **2004**, *126*, 984–985. (c) Zeis, R.; Siegrist, T.; Kloc, Ch. *Appl. Phys. Lett.* **2005**, *86*, 022103. (d) Briseno, A. L.; Mannsfeld, S. C. B.; Ling, M. M.; Liu, S.; Tseng, R. J.; Reese, C.; Roberts, M. E.; Yang, Y.; Wudl, F.; Bao, Z. *Nature* **2006**, *444*, 913–917. (e) Reese, C.; Bao, Z. *J. Mater. Chem.* **2006**, *16*, 329–333. (f) Briseno, A. L.; Mannsfeld, S. C. B.; Reese, C.; Hancock, J. M.; Xiong, Y.; Jenekhe, S. A.; Bao, Z.; Xia, Y. *Nano Lett.* **2007**, *7*, 2847–2853.

(3) (a) Kim, D. H.; Han, J. T.; Park, Y. D.; Jang, Y.; Cho, J. H.; Hwang, M.; Cho, K. *Adv. Mater.* **2006**, *18*, 719–723. (b) Briseno, A. L.; Mannsfeld, S. C. B.; Shamberger, P. J.; Ohuchi, F. S.; Bao, Z.; Jenekhe, S. A.; Xia, Y. *Chem. Mater.* **2008**, *20*, 4712–4719.

(4) (a) Zhang, X.; Zhang, J.; Song, W.; Liu, Z. *J. Phys. Chem. B* **2006**, *110*, 1158–1165. (b) Huang, J.; Kaner, R. B. *J. Am. Chem. Soc.* **2004**, *126*, 851–855. (c) Maynor, B. W.; Filocamo, S. F.; Grinstaff, M. W.; Liu, J. *J. Am. Chem. Soc.* **2002**, *124*, 522–523. (d) Li, D.; Xia, Y. N. *Adv. Mater.* **2004**, *16*, 1151–1170. (e) O'Brien, G. A.; Quinn, A. J.; Tanner, D. A.; Redmond, G. *Adv. Mater.* **2006**, *18*, 2379–2383. (f) Liu, J.; Lin, Y.; Liang, L.; Voigt, J. A.; Huber, D. L.; Tian, Z. R.; Coker, E.; Mckenzie, B.; Mcdermott, M. J. *Chem.—Eur. J.* **2003**, *9*, 604–611. (g) Kim, H.; Park, Y. D.; Jang, Y.; Kim, S.; Cho, K. *Macromol. Rapid Commun.* **2005**, *26*, 834–839. (h) Aleshin, A. N. *Adv. Mater.* **2006**, *18*, 17–27. (i) Schenning, A. P. H. J.; Meijer, E. W. *Chem. Commun.* **2005**, 3245–3258.

Scheme 1. Molecular Structure of TA-PPE

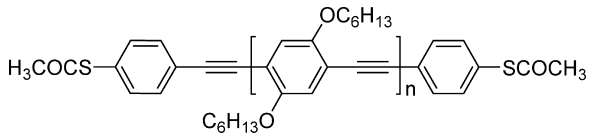

ments for the formation of high-quality, crystalline 1D polymer nanowires, such as the successful examples of poly(3-hexylthiophene) (P3HT) and poly(benzobisimidazobenzophenanthroline) (BBL).[3] Here, we show the preparation of high quality 1D nanowires using another class of conjugated polymer materials, poly(*para*-phenylene ethynylene)s (PPEs). PPEs, an important kind of polymer semiconductor, exhibit not only excellent optoelectronic and nonlinear optical properties but also high thermal and oxidative stability as well as photostability, which makes them attractive in many research fields, for example in polymer light-emitting diodes, sensors, flat panel displays, and other devices.[5] Additionally, the special rigid-rod conjugated conformation[6] as well as good conductivity[5a,7] of PPEs has stimulated increasing interest in their utilization in nanochemistry as building blocks for nanodevices, such as the pioneered works performed by Samori, Rabe, Müllen, Bunz and other distinguished scientists,[8] and various nanostructures of PPEs such as nanoribbons, nanotubes, and nanotowers, etc. were generated. Although it is expected that these PPEs nanostructures may exhibit very unique properties and lead to advancement of performance for devices, until now their applications in devices have rarely been addressed and the structure and properties of these nanostructures are still unclear. Thus, it will be attractive and imperative to examine the structure and property of the nanostructures to guide the growth of high quality, single crystalline 1D nanowires of the polymers and further extend them for potential applications in nanodevices. Here, a derivative of PPEs, a poly(*para*-phenylene ethynylene) derivative with thioacetate end groups (TA-PPE)[9] as shown in Scheme 1, was used as the candidate to approach this target. Large-area, well-defined nanowires of TA-PPE were controllably assembled. X-ray diffraction (XRD) and transmission electron microscopy (TEM) demonstrated that TA-PPE nanowires exhibited high crystalline characteristics in an orthorhombic crystal unit cell with lattice parameters of $a \approx 13.63$ Å, $b \approx 7.62$ Å, and $c \approx 5.12$ Å. Moreover, organic field-effect transistors (OFETs) based on the nanowires exhibited the highest charge carrier mobility approaching 0.1 $cm^2/(V\ s)$, which was 3−4 orders higher than that of thin film transistors of the same polymer, indicating the high performance of the 1D polymer nanowire crystals and their potential applications in organic electronic and nanoelectronic devices.

Experimental Section

TA-PPE was synthesized by the polymerization of 1,4-diethynyl-2,5-bis(hexyloxy)benzene (M1) and 1,4-bis(hexyloxy)-2,5-diiodobenzene (M2) through a Sonogashira Pd−Cu coupling reaction.[10] ^{1}H and ^{13}C NMR data of TA-PPE were shown as follows: ^{1}H NMR (400 MHz, $CDCl_3$, 25 °C) data: δ = 7.01 (bs), 4.02−4.05 (m), 2.44 (m, end group), 1.82−1.89 (m), 1.51−1.54 (m), 1.34−1.35 (m), 0.89−0.91 (m). ^{13}C NMR (600 MHz, $CDCl_3$, 25 °C) data: δ =153.55 (Ar−O), 117.31 (Ar−H), 114.36 (Ar−C≡), 91.62 (C≡C), 69.73 (−OCH_2), 31.65 (CH_2), 29.33 (CH_2), 25.71 (CH_2), 22.66 (CH_2), 14.06 (CH_3). The ^{1}H NMR peak at ∼2.44 ppm of the obtained products confirmed the existence of the end group (−$SCOCH_3$). The molecular weight (M_w) of our TA-PPE was ∼51 328 g/mol with a polydispersity (D) of 3.09, which was estimated by gel permeation chromatography (GPC) with polystyrene as the calibration standard and tetrahydrofuran (THF) as the eluent at room temperature. The detailed synthesis procedure, the spectra of ^{1}H and ^{13}C NMR, and the GPC data of our TA-PPE were further given in the Supporting Information (see Supporting Information 1).

TA-PPE nanowires were produced by slowly self-assembling from a solution (0.05−1.0 mg/mL) under a certain solvent pressure in a closed jar, which could be depicted by Figure 1. It should be noted that the solvent in the bottom of the jar was very crucial for the formation of well-defined TA-PPE nanowires, which could play two important roles: (1) slow evaporation of the solvent guaranteed the polymer molecules had sufficient time to adjust themselves and come together with strong intermolecular interactions and further self-assembled into crystalline nanowires on the substrate; (2) certain solvent vapor pressure in the upper space of the jar could guarantee the free movement of the polymer molecules and then induced them to assemble together leading to the growth of nanowires. Due to the good solubility of TA-PPE molecules, tetrahydrofuran (THF), toluene, and chlorobenzene, etc. have been used as the solvent, and the results demonstrated that THF was the optimum choice for the preparation of desired TA-PPE nanowire crystals due to its good volatility and the high solvent vapor pressure in the upper space of the jar. With the self-assembly of TA-PPE in

(5) (a) Bunz, U. H. F. *Chem. Rev.* **2000**, *100*, 1605–1644. (b) Xu, Y. F.; Berger, P. R.; Wilson, J. N.; Bunz, U. H. F. *Appl. Phys. Lett.* **2004**, *85*, 4219–4221. (c) Schmitz, C.; Pösch, P.; Thelakkat, M.; Schmidt, H.-W.; Montali, A.; Feldman, K.; Smith, P.; Weder, C. *Adv. Funct. Mater.* **2001**, *11*, 41–46. (d) Chu, Q.; Pang, Y.; Ding, L.; Karasz, F. E. *Macromolecules* **2002**, *35*, 7569–7574. (e) Pschirer, N. G.; Miteva, T.; Evans, U.; Roberts, R. S.; Marshall, A. R.; Neher, D.; Myrick, M. L.; Bunz, U. H. F. *Chem. Mater.* **2001**, *13*, 2691–2696. (f) McQuade, D. T.; Pullen, A. E.; Swager, T. M. *Chem. Rev.* **2000**, *100*, 2537–2574. (g) Breen, C. A.; Deng, T.; Breiner, T.; Thomas, E. L.; Swager, T. M. *J. Am. Chem. Soc.* **2003**, *125*, 9942–9943. (h) Weder, C.; Sarwa, C.; Montali, A.; Bastiaansen, C.; Smith, P. *Science* **1998**, *279*, 835–837.

(6) (a) Moroni, M.; Le Moigne, J.; Luzzati, S. *Macromolecules* **1994**, *27*, 562–571. (b) Wautelet, P.; Moroni, M.; Oswald, L.; Le Moigne, J.; Pham, A.; Bigot, J.-Y. *Macromolecules* **1996**, *29*, 446–455.

(7) (a) Kokil, A.; Shiyanovskaya, I.; Singer, K. D.; Weder, C. *J. Am. Chem. Soc.* **2002**, *124*, 9978–9979. (b) Kokil, A.; Shiyanovskaya, I.; Singer, K. D.; Weder, C. *Synth. Met.* **2003**, *138*, 513–517.

(8) (a) Samori, P.; Francke, V.; Mangel, T.; Müllen, K.; Rabe, J. P. *Opt. Mater.* **1998**, *9*, 390–393. (b) Samori, P.; Francke, V.; Müllen, K.; Rabe, J. P. *Thin Solid Films* **1998**, *336*, 13–15. (c) Samori, P.; Sikharulidze, I.; Francke, V.; Müllen, K.; Rabe, J. P. *Nanotechnology* **1999**, *10*, 77–80. (d) Samori, P.; Francke, V.; Müllen, K.; Rabe, J. P. *Chem.—Eur. J.* **1999**, *5*, 2312–2317. (e) Perahia, D.; Traiphol, R.; Bunz, U. H. F. *Macromolecules* **2001**, *34*, 151–155. (f) Xu, J.; Zhou, C.-Z.; Yang, L. H.; Chung, N. T. S.; Chen, Z.-K. *Langmiur* **2004**, *20*, 950–956. (g) Traiphol, R.; Perahia, D. *Thin Solid Films* **2006**, *515*, 2123–2129. (h) Mio, M. J.; Prince, R. B.; Moore, J. S.; Kuebel, C.; Martin, D. C. *J. Am. Chem. Soc.* **2000**, *122*, 6134–6135. (i) Wilson, J. N.; Bangcuyo, C. G.; Erdogan, B.; Myrick, M. L.; Bunz, U. H. F. *Macromolecules* **2003**, *36*, 1426–1428.

(9) (a) Hu, W.; Nakashima, H.; Furukawa, K.; Kashimura, Y.; Ajito, K.; Liu, Y.; Zhu, D.; Torimitsu, K. *J. Am. Chem. Soc.* **2005**, *127*, 2804–2805. (b) Hu, W.; Jiang, J.; Nakashima, H.; Luo, Y.; Kashimura, Y.; Chen, K.; Shuai, Z.; Furukawa, K.; Lu, W.; Liu, Y.; Zhu, D.; Torimitsu, K. *Phys. Rev. Lett.* **2006**, *96*, 027801. (c) Hu, W.; Nakashima, H.; Furukawa, K.; Kashimura, Y.; Ajito, K.; Torimitsu, K. *Appl. Phys. Lett.* **2004**, *85*, 115. (d) Hu, W.; Nakashima, H.; Furukawa, K.; Kashimura, Y.; Ajito, K.; Han, C.; Torimitsu, K. *Phys. Rev. B* **2004**, *69*, 165207. (e) Dong, H.; Li, H.; Wang, E.; Wei, Z.; Xu, W.; Hu, W.; Yan, S. *Langmuir* **2008**, *24*, 13241–13244. (f) Dong, H.; Li, H.; Wang, E.; Nakashima, H.; Torimitsu, K.; Hu, W. *J. Phys. Chem. C* **2008**, *112*, 19690–19693. (g) Dong, H.; Li, H.; Wang, E.; Yan, S.; Zhang, J.; Yang, C.; Takhashi, I.; Nakashima, H.; Torimitsu, K.; Hu, W. *J. Phys. Chem. B* **2009**, *113*, 4176–4180.

(10) (a) Nakashima, H.; Furukawa, K.; Kashimura, Y.; Torimitsu, K. *Polym. Prepr. (Am. Chem. Soc. Div. Polym. Chem.)* **2003**, *44*, 482–483. (b) Nakashima, H.; Furukawa, K.; Ajito, K.; Kashimura, Y.; Torimitsu, K. *Langmuir* **2005**, *21*, 511–515.

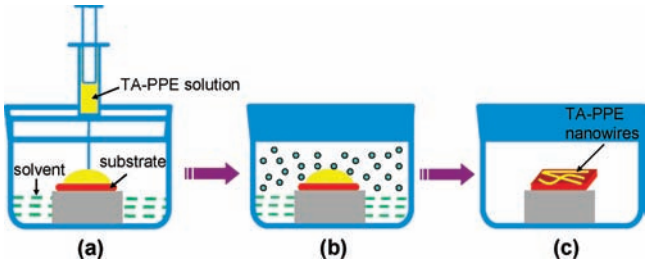

Figure 1. Schematics for the preparation of TA-PPE nanowires: (a) injecting a drop of TA-PPE solution onto the substrate, which is in the jar with solvent in the bottom, (b) TA-PPE molecules self-assembling into nanowires in the solvent atmosphere, (c) large-area TA-PPE nanowires obtained on the substrate after self-assembling for 2−3 days.

the closed jar for ∼2−3 days, large-area, well-defined TA-PPE nanowires could be obtained. Then, the resulted products were dried in a vacuum oven for 4 h at 60 °C to remove the residual solvent prior to characterizations.

The morphologies of TA-PPE nanowires were characterized by a fluorescent microscope (Cary Eclipse fluorescence spectrophotometer) with an exposure time of 1 s under 400 nm excitation, scanning electron microscopy (SEM, Hitachi S-4300 SE), atomic force microscopy (AFM, Digital Instrument, Nanoscopy IIIa) with commercially silicon cantilevers in a tapping mode, X-ray diffraction (XRD, D/max2500) by the usual $\theta-2\theta$ method with a 40 KV voltage and a Cu Kα source (λ = 1.541 Å), and transmission electron microscopy (TEM, Hitachi H-800) operated at 100 kV. The SEM images were taken at 15.0 kV with gold sputtered samples. The samples for TEM measurement were prepared by floating TA-PPE nanowires onto a distilled water surface from a carbon-coated mica substrate and then transferred onto the copper grids. To reduce the damage of the electron beam to the polymer samples, the focusing beam was carried out on a specific area and then the specimen film was translated to its adjacent undamaged area with its image recorded immediately.

Top-contacted OFETs based on the TA-PPE nanowires were constructed on a Si/SiO_2 substrate (*n*-type Si wafer containing 500 nm-thick SiO_2, capacitance = 7.5 nF/cm^2) using an "organic ribbon mask" technique.[11] Prior to the self-assembly of TA-PPE nanowires, the Si/SiO_2 substrate was cleaned with pure water, a hot concentrated sulfuric acid−hydrogen peroxide solution (concentrated sulfuric acid/hydrogen peroxide water = 2:1), pure water, pure ethanol, and pure acetone, successively. Then, TA-PPE nanowires were produced on Si/SiO_2 substrates through the self-assembling method as mentioned in the above section. Subsequently, 30 nm thick source and drain electrodes were deposited on the nanowires by thermal evaporation with an organic ribbon as the mask. For comparison top-contacted OFET devices based on 70−100 nm TA-PPE thin films were constructed under the same experimental conditions. The channel length and width of the thin-film transistors were 0.1 and 4.82 mm, respectively. Electrical characteristics of the transistors were recorded by a Keithley 4200 SCS with a Micromanipulator 6150 probe station in a clean and shielded box at room temperature in air.

Results and Discussion

The assembled products of TA-PPE were shown in Figure 2, which demonstrated well-defined 1D nanowires with a length from several to tens micrometers long. The concentration of the TA-PPE solution for self-assembly would change the density of the polymer nanowire networks greatly, but with little influence on the diameter of the nanowires (Figure 2a−c), indicating the intrinsic nature of the polymer molecules for self-assembly. As shown in Figure 2a, when the solution concentration of TA-PPE was at ∼1.0 mg/mL the density of the polymer nanowires was rather high, so that they easily formed network structures. If the solution concentration of TA-PPE was over 1.0 mg/mL, a multilayer nanowire network would be generated. With the concentration of the polymer solution decreasing (<1.0 mg/mL), the density of the nanowires would decrease too (Figure 2b and c), so that the accurate control of the self-assembly process for the generation of the polymer nanowires became accessible. For example, as shown in Figure 2c, when the solution concentration of the TA-PPE was at ∼0.1 mg/mL, low density and well-dispersed TA-PPE nanowires could be easily obtained on the substrates. Furthermore, with the low concentration for self-assembly, long polymer nanowires with tens or hundreds of micrometers in length could be obtained as shown in Figure 2d and e.

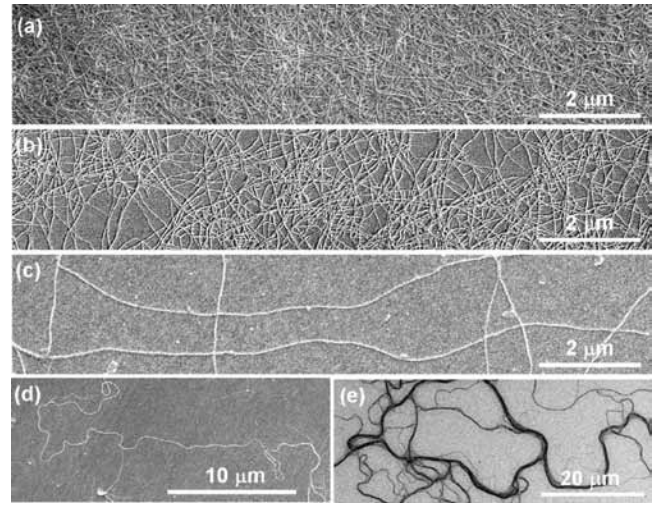

Figure 2. SEM images of the self-assembled TA-PPE nanowires on Si/SiO_2 substrates from THF solution: (a) ∼1.0 mg/mL, (b) ∼0.5 mg/mL, (c) ∼0.1 mg/mL, (d) an individual nanowire tens of micrometers long, (e) bundles of nanowires hundreds of micrometers long.

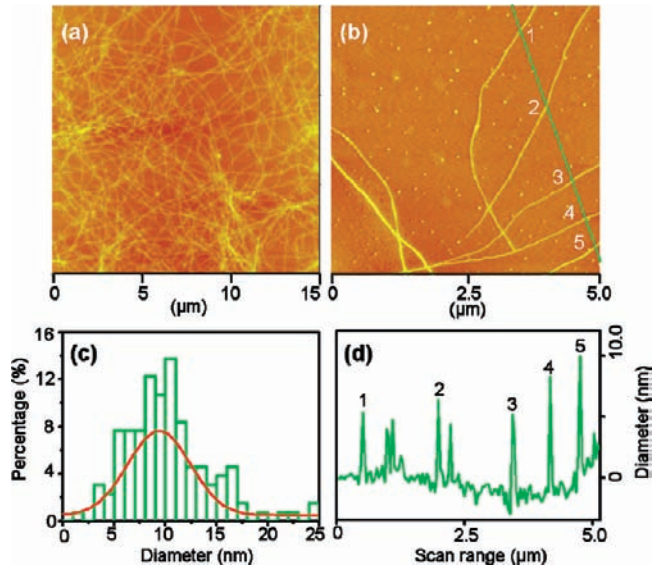

Figure 3. (a, b) AFM images of self-assembled TA-PPE nanowires on Si/SiO_2 substrates from THF solution (0.5 mg/mL). (c,d) Diameter distribution of the self-assembled nanowires.

AFM images of the well-defined TA-PPE nanowires were shown in Figure 3a and b. The results confirmed the uniform

(11) Jiang, L.; Gao, J.; Wang, E.; Li, H.; Wang, Z; Hu, W.; Jiang, L. *Adv. Mater.* **2008**, *20*, 2735–2740.

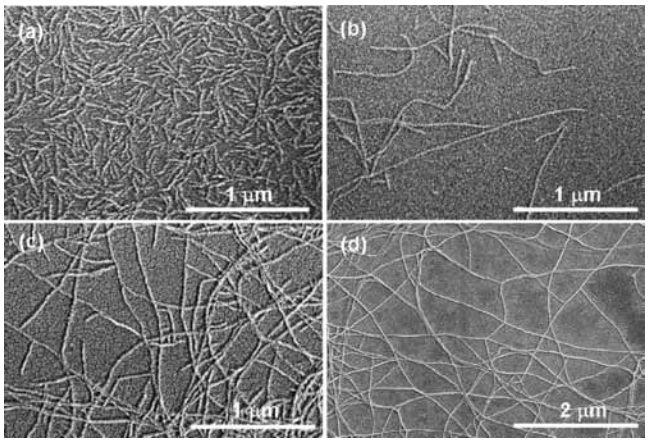

Figure 4. SEM images of the growth processes of the self-assembled TA-PPE rigid polymer nanowires.

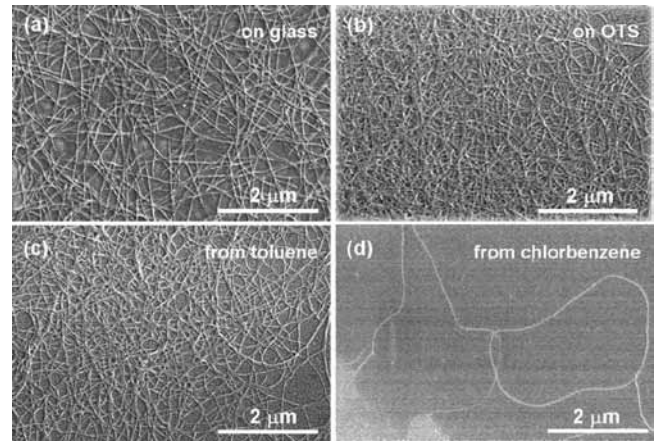

Figure 5. SEM images of the self-assembled TA-PPE nanowires on (a) glass and (b) OTS substrates from THF solution, and from (c) toluene and (d) chlorobenzene solution on Si/SiO_2 substrates.

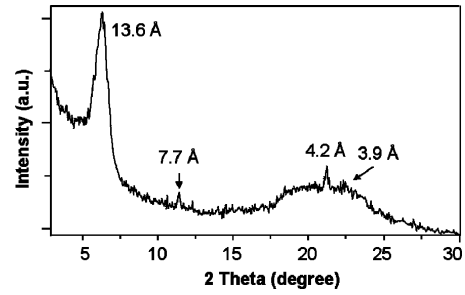

Figure 6. XRD pattern of the self-assembled TA-PPE nanowires, indicating the formation of typical lamellar structure of the nanowires with interlayer *d*-spacing of 13.63 Å (at $2\theta = 6.48°$).

self-assembled products of the rigid conjugated polymer. The diameter of the nanowires was mainly ~5−15 nm (Figure 3c and d). For a given individual TA-PPE nanowire its diameter along the nanowire long axis was nearly constant (see Supporting Information 2), which further confirmed the regular and well-defined molecular packing in the polymer nanowires. The highly uniform polymer nanowires provided a vivid example of the controllable assembly of conjugated polymer nanostructures for potential application in nanodevices.

The growth process of the nanowires was pursued by a "step-by-step" growth mechanism. Originally, TA-PPE molecules formed very short nanorods on substrates as shown in Figure 4a. Fortunately, the vapor pressure of the solvent allowed for free movement of TA-PPE molecules on the substrate, so that the short TA-PPE nanorods grew step-by-step to form longer nanorods even nanowires as shown in Figure 4b. With continuation of the growth process, the polymer nanowires would further grow into longer nanowires (Figure 4c) and finally evolve into beautiful nanowire networks as shown in Figure 4d. These results provided direct proof for the growth of TA-PPE nanowires and were further beneficial for the interpretation of the structure of the conjugated polymer nanowires.

The self-assembly of TA-PPE nanowires exhibited no obvious substrate dependence, regardless if the substrate used was glass, quartz, SiO_2, or octadecyltrichlorosilan (OTS)-modified Si/SiO_2 substrate; beautiful nanowires were obtained as exemplified in Figure 5a and b. Similarly, the solvent effect on the self-assembly process was also investigated. It was found that the best candidate solvents for TA-PPE self-assembly were THF and toluene (Figure 5a−c). Although nanowires of TA-PPE were also found by using chlorobenzene, CH_2Cl_2, and $CHCl_3$ as solvents (as exemplified in Figure 5d), the products were much worse than the nanowires from THF and toluene, and the solvent selection rule seemed to be toluene ≈ THF > chlorobenzene > $CHCl_3$ > CH_2Cl_2. Considering the polarity of the solvents is CH_2Cl_2 > $CHCl_3$ > chlorobenzene > THF > toluene, the results indicated the solvent polarity played a key role for the self-assembly of TA-PPE nanowires. The weak substrate dependence and the strong solvent dependence would be meaningful for the controllable assembly of the rigid conjugated polymer nanowires and further extension of their potential applications in devices.

To acquire a better understanding of the crystal structure and molecular packing in TA-PPE nanowires, XRD measurement was carried out on the TA-PPE nanowires. Figure 6 showed the XRD pattern of self-assembled TA-PPE nanowires. It was obvious that a strong and sharp diffraction peak at $2\theta = 6.48°$ was observed, which arose from the ordered interlayer packing of TA-PPE molecules. Other prominent reflection peaks at $2\theta = 11.42°$, 21.14°, and 22.3° were also observed for TA-PPE nanowires, which originated from the $\pi-\pi$ interchain stacking of the conjugated polymer main chains. The presence of these distinct diffraction peaks suggested the formation of typical lamellar structure of the nanowires with an interlayer *d*-spacing of 13.63 Å (at $2\theta = 6.48°$).[12]

These prominent and sharp diffraction peaks reflected the appreciable crystallinity of the TA-PPE nanowires, which was further confirmed by their transmission electron microscopy (TEM) results. Figure 7a and 7b exhibited the TEM image of an individual TA-PPE nanowire and its corresponding selected-area electron diffraction (SAED) pattern. Interestingly, the TA-PPE nanowires exhibited single crystalline characteristics with three obvious diffraction peaks at 3.81, 4.27, and 2.56 Å. In combination with the XRD diffraction pattern as shown in Figure 6, the absence of the 13.63 Å peak indicated that the TA-PPE molecules lay on the support plane with the side chains standing on the substrate. Additionally, the diffraction peak of 3.81 Å was in good agreement with the close interchain distance

(12) (a) Ofer, D.; Swager, T. M.; Wrighton, M. S. *Chem. Mater.* **1995**, *7*, 418–425. (b) Weder, C.; Wrighton, M. S. *Macromolecules* **1996**, *29*, 5157–5165. (c) Weder, C.; Wrighton, M. S.; Spreiter, R.; Bosshard, C.; Günter, P. *J. Phys. Chem.* **1996**, *100*, 18931–18936. (d) Bunz, U. H. F.; Enkelmann, V.; Kloppenburg, L.; Jones, D.; Shimizu, K. D.; Claridge, J. B; zur Loye, H.-C.; Lieser, G. *Chem. Mater.* **1999**, *11*, 1416–1424.

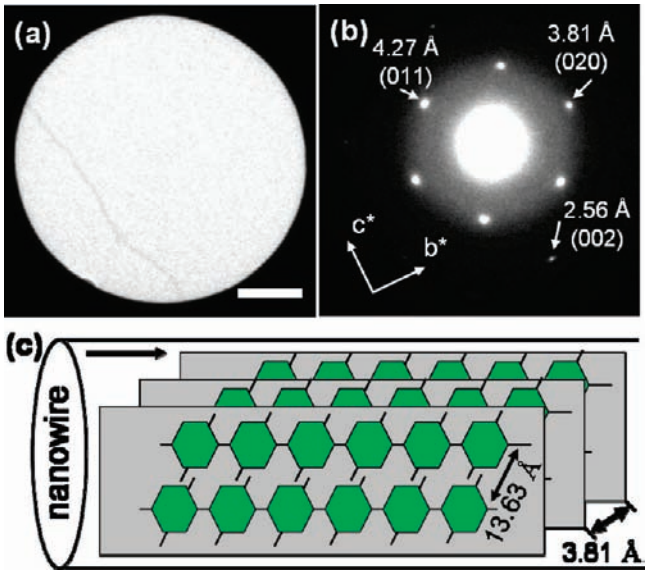

Figure 7. (a) TEM image of an individual TA-PPE nanowire (scale bar: 150 nm) and (b) its corresponding SAED pattern. (c) Schematic diagram of possible molecular packing in the one-dimensional nanowires; for clarity the end-capping groups have been omitted.

(3.7−3.8 Å) of $\pi-\pi$ stacking between the two adjacent main chains, which was nearly perpendicular to the nanowire long axis (~10° discrepancy induced by the imaging system of TEM used), indicating that $\pi-\pi$ stacking direction in TA-PPE nanowires was predominantly perpendicular to the long axis of the nanowires. Hence, the molecular packing in the nanowires could be depicted in Figure 7c (for simplicity, the end-capping groups were omitted in the schematic diagram of molecular packing of the nanowires). A similar molecular packing motif has been found for the crystalline strands of chirally substituted PPEs,[13] wherein the PPEs molecules were oriented in a staggered array with the chain backbones aligning along the long axis of the strands. However, different from the triclinic unit cell of the chiral PPEs strands,[13] here our TA-PPE nanowires exhibited a typical orthorhombic crystal unit cell with lattice parameters of $a \approx 13.63$ Å, $b \approx 7.62$ Å, and $c \approx 5.12$ Å probably due to the high symmetry structure of TA-PPE molecules.

These well-defined, crystalline nanowires provided a great advantage for the examination of intrinsic properties of the rigid polymer as well as the fabrication of high performance devices based on the nanowire crystals. As an example, transport properties of the nanowires were examined by OFETs. The devices could be fabricated by both bottom-contact and top-contact device configurations. Bottom-contact devices were fabricated by first predepositing electrode arrays on Si/SiO_2 substrates with photolithography, with TA-PPE nanowires self-assembling between the electrodes (see Supporting Information 3). Top-contact devices were constructed by depositing Au gap electrodes on the nanowires through an "organic ribbon mask" technique[11] (Figure 8a and b), which was performed on a Micromanipulator 6150 probe station with a high resolution microscopy (magnification at 400−1000 times). The fabrication of the top-contact devices could be described as follows: (i) growth of TA-PPE nanowires on substrates, (ii) an organic microwire was picked up by the mechanical probe of the

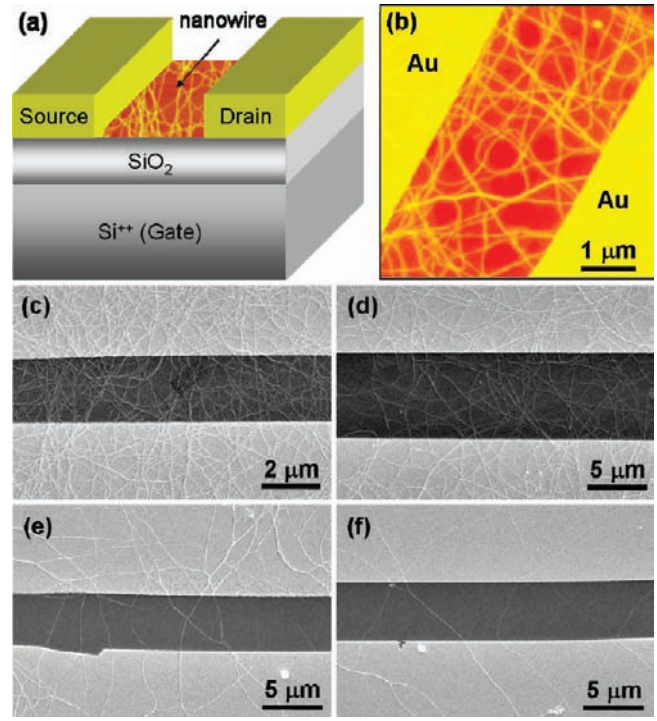

Figure 8. OFETs of TA-PPE nanowires fabricated by "organic ribbon mask" technique, (a) schematic diagram of the top contact devices, (b) AFM image of a representative device, (c−f) SEM images of the transistor devices with different density of nanowires between the source and drain electrodes.

Micromanipulator 6150 probe station and laminated across the nanowires as a mask, (iii) Au electrodes (source and drain) were vacuum evaporated on the masked structure, and (iv) the masked microwire was peeled off by the mechanical probe again. The top-contact devices can effectively avoid the contact problem between electrodes and polymer nanowires and improve the device performance; hence, the top-contact device was preferred by us here. By using this simple and facile device fabrication technique,[11] different densities of TA-PPE nanowires in the conducting channel could be fabricated and examined carefully (Figure 8c−f).

The typical output and transfer characteristics of an exemplified transistor are shown in Figure 9a and b. It is obvious that the TA-PPE nanowire device exhibits excellent p-type transistor behavior with well-resolved saturation currents at a gate voltage of −40 V. For mobility calculations, SEM and AFM were conducted to define the channel length and width and the number of TA-PPE nanowires bridging the source and drain electrodes after measuring the device properties. Then the saturated field-effect transistor mobilities were calculated by using the following equation:[14]

$$I_{DS,sat} = (WC_{i\mu sat}/2L)(V_G - V_T)^2$$

where W is the channel width (here refer to the width of the nanowires bridging the source and drain electrodes), L is the channel length, respectively, C_i is the capacitance per unit area of the gate insulator, μ_{sat} is the field-effect mobility in the saturated region, V_G is the gate voltage, and V_T is the threshold voltage.

(13) Wilson, J. N.; Steffen, W.; McKenzie, T. G.; Lieser, G.; Oda, M.; Neher, D.; Bunz, U. H. F. *J. Am. Chem. Soc.* **2002**, *124*, 6830–6831.

(14) Sze, S. M. *Physics of Semiconductor Devices*, 2nd ed.; Wiley: New York, 1981.

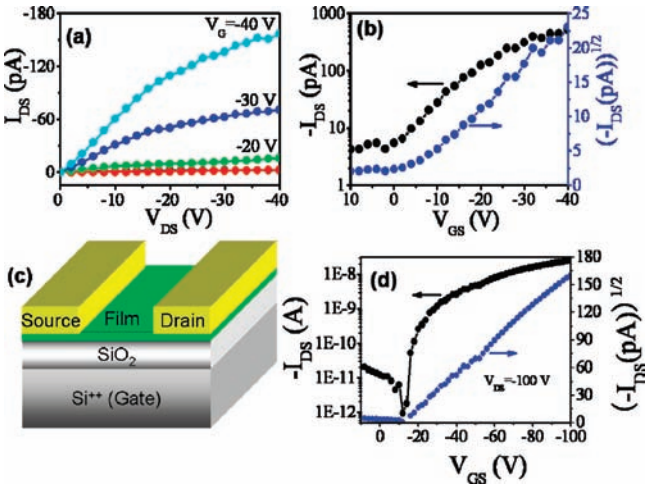

Figure 9. (a-b) Typical output and transfer characteristics of an exemplified device with channel width at ~2−3 μm, length: ~2.63 μm, (c) schematic diagram of TA-PPE thin film transistors, (d) typical transfer characteristics of TA-PPE thin film transistors with channel length and width at 0.1 and 4.82 mm, respectively.

According to the transfer characteristics, the average field-effect mobilities (μ) of the TA-PPE nanowire transistors were estimated to be $\sim 10^{-2}$ cm^2/(V s), and the highest mobility reached 0.1 cm^2/(V s). It is well-known that the high disorder of polymer films limits the carrier transport so that the mobility of polymer films is usually low. For example, thin film transistors of TA-PPE were also fabricated and characterized under the same conditions as those shown in Figure 9c and d. The typical transistor behavior (Figure 9d) suggested the thin film mobilities were between $\sim 10^{-5}$ cm^2/(V s) and $\sim 10^{-6}$ cm^2/(V s). The field-effect mobilities observed from nanowire crystals were more than 3−4 orders of magnitude higher than that observed from its thin films, indicating the high quality of the one-dimensional polymer nanowire crystals. Moreover, considering the $\pi-\pi$ stacking direction in TA-PPE nanowires was predominantly perpendicular to the long axis of the nanowires, the results definitely validated the efficient charge transport along the polymer nanowires, i.e., along the polymer backbone chain direction. The results opened the prospect for efficient charge carrier mobilities of PPEs derivatives[7a,b] as well as the potential applications of the polymer for advancement in OFETs.

Conclusions

In conclusion, we have produced large-area and well-defined TA-PPE nanowires by self-assembly from a dilute solution. Structural analyses demonstrated that in the nanowires the backbones of TA-PPE chains were parallel to the nanowire long axis with their side chains standing on the substrate. These well-defined, highly crystalline TA-PPE polymer nanowires demonstrate potential applications in nanodevices. And as an example of their potentianl applications in devices, OFETs based on the TA-PPE nanowires were fabricated and the transport properties of the nanowires examined by OFETs suggested the average charge carrier mobilities of the polymer crystalline nanowire transistors were $\sim 10^{-2}$ cm^2/(V s) and the highest mobility could reach 0.1 cm^2/(V s), which was ~3−4 orders higher than that of its thin film transistors under the same conditions. To our knowledge, it is the first example of PPEs' crystalline transistors, and here these results further advance PPEs as promising semiconducting materials in applications of organic electronic and nanoelectronic devices.

Acknowledgment. The authors are grateful to the profound discussions with Prof. Alan Heeger and the financial support from NSFC (20721061, 20872146, 50725311, and 50828301), NSFC-DFG TRR61, Ministry of Science and Technology of China (2006CB932100, 2006CB806200), and Chinese Academy of Sciences.

Supporting Information Available: The synthesis and characterizations of TA-PPE polymer, TA-PPE nanowires, bottom contact TA-PPE nanowires devices, these information are available free of charge via the Internet at http://pubs.acs.org.

JA907015P